

Hypocalcemia-Induced Slowing of Human Sinus Node Pacemaking

Axel Loewe,^{1,*} Yannick Lutz,¹ Deborah Nairn,¹ Alan Fabbri,^{2,3} Norbert Nagy,⁴ Noemi Toth,⁴ Xiaoling Ye,⁵ Doris H. Fuertinger,⁵ Simonetta Genovesi,⁶ Peter Kotanko,^{5,7} Jochen G. Raimann,⁵ and Stefano Severi²

¹Institute of Biomedical Engineering, Karlsruhe Institute of Technology (KIT), Karlsruhe, Germany; ²Department of Electrical, Electronic and Information Engineering “Guglielmo Marconi,” University of Bologna, Cesena, Italy; ³Department of Medical Physiology, University Medical Center Utrecht, Utrecht, The Netherlands; ⁴Department of Pharmacology and Pharmacotherapy, University of Szeged, Szeged, Hungary; ⁵Renal Research Institute, New York City, New York; ⁶Department of Medicine and Surgery, Università degli Studi di Milano-Bicocca, Monza, Italy; and ⁷Icahn School of Medicine at Mount Sinai, New York City, New York

ABSTRACT Each heartbeat is initiated by cyclic spontaneous depolarization of cardiomyocytes in the sinus node forming the primary natural pacemaker. In patients with end-stage renal disease undergoing hemodialysis, it was recently shown that the heart rate drops to very low values before they suffer from sudden cardiac death with an unexplained high incidence. We hypothesize that the electrolyte changes commonly occurring in these patients affect sinus node beating rate and could be responsible for severe bradycardia. To test this hypothesis, we extended the Fabbri et al. computational model of human sinus node cells to account for the dynamic intracellular balance of ion concentrations. Using this model, we systematically tested the effect of altered extracellular potassium, calcium, and sodium concentrations. Although sodium changes had negligible (0.15 bpm/mM) and potassium changes mild effects (8 bpm/mM), calcium changes markedly affected the beating rate (46 bpm/mM ionized calcium without autonomic control). This pronounced bradycardic effect of hypocalcemia was mediated primarily by I_{CaL} attenuation due to reduced driving force, particularly during late depolarization. This, in turn, caused secondary reduction of calcium concentration in the intracellular compartments and subsequent attenuation of inward I_{NaCa} and reduction of intracellular sodium. Our *in silico* findings are complemented and substantiated by an empirical database study comprising 22,501 pairs of blood samples and *in vivo* heart rate measurements in hemodialysis patients and healthy individuals. A reduction of extracellular calcium was correlated with a decrease of heartrate by 9.9 bpm/mM total serum calcium ($p < 0.001$) with intact autonomic control in the cross-sectional population. In conclusion, we present mechanistic *in silico* and empirical *in vivo* data supporting the so far neglected but experimentally testable and potentially important mechanism of hypocalcemia-induced bradycardia and asystole, potentially responsible for the highly increased and so far unexplained risk of sudden cardiac death in the hemodialysis patient population.

SIGNIFICANCE We propose a pathomechanism potentially responsible for the >10,000 yearly sudden cardiac deaths in hemodialysis patients. Using a computational model of human sinus node cells, we show how a reduction of extracellular calcium causes severe slowing of spontaneous sinus node beating by attenuation of I_{CaL} , particularly during late diastolic depolarization. Secondary reduction of calcium in the intracellular compartments and subsequent attenuation of inward I_{NaCa} and reduction of intracellular sodium occurs. These findings are substantiated by an *in vivo* analysis of >22,000 blood samples showing a highly significant bradycardic effect of hypocalcemia. In conclusion, we present mechanistic *in silico* and empirical *in vivo* data supporting the experimentally testable hypothesis of hypocalcemia-induced bradycardia, potentially responsible for sudden cardiac death in hemodialysis patients.

INTRODUCTION

The heart is driven by regular excitations generated in the sinus node as the natural pacemaker. The spontaneous

beating of sinus node myocytes and its rate is governed by a delicate balance of inward and outward transmembrane currents in the diastolic depolarization (DD) phase of the action potential (AP) and the intricate interplay of the calcium and membrane clocks, known as the coupled clock mechanism (1,2). A key factor affecting sinus node cellular electrophysiology is the extracellular milieu, which is tightly controlled in mammals. Among other functions, the kidneys

Submitted March 21, 2019, and accepted for publication July 24, 2019.

*Correspondence: publications@ibt.kit.edu

Editor: Kenneth Campbell.

<https://doi.org/10.1016/j.bpj.2019.07.037>

© 2019 Biophysical Society.

play a crucial role in maintaining homeostasis and keeping electrolyte concentrations in the blood and the extracellular milieu within narrow ranges. In end-stage renal disease (ESRD) patients undergoing hemodialysis (HD), however, the renal system fails to maintain electrolyte homeostasis, with consequences for several other organ systems, including the heart and its electrical conduction system with the sinus node as the intrinsic natural pacemaker. The ESRD population is large, with >700,000 patients in Europe alone (3).

A particularly severe complication is sudden cardiac death (SCD), which is abnormally frequent in the HD population. Indeed, the SCD-related mortality is increased 14-fold in ESRD patients undergoing HD when compared to subjects with a history of cardiovascular disease and normal kidney function (4). Traditional cardiovascular risk factors do not explain the exceptionally high rate of SCD in HD patients (4,5). Although the most common pathomechanisms underlying SCD in the general population are tachyarrhythmias (ventricular tachycardia, ventricular fibrillation), several independent studies recently indicated that bradycardia and asystole are likely to be the dominant pathomechanisms of SCD in ESRD patients. Wong et al. implanted cardiac monitors in 50 HD patients (6). The monitors could be interrogated in six patients who died from SCD in the 18 ± 4 months of the follow-up period. All these patients died from severe bradycardia followed by asystole, and none of them showed ventricular tachyarrhythmia before or after bradycardic events (6). All SCDs occurred in the long interdialytic period, suggesting a major role for accumulation or depletion of certain substances between dialysis sessions affecting the electrical pacemaking and conduction system of the heart as a key pathomechanism. To date, the actual pathomechanism behind the unexplained high rate of SCD in HD patients has remained elusive (4,7), and very recently, unconventional ideas like plastic chemical exposure were put forward (8). Interestingly, the findings by Wong et al. were confirmed and complemented by other studies collectively comprising 317 dialysis patients as recently reviewed (7,9). These in vivo data indicate that bradycardia and asystole are more frequent than ventricular fibrillation as a cause of SCD in ESRD patients and led us to hypothesize that there is a role of the cardiac pacemaking system and that spontaneous sinus node beating rate in humans is modulated to a degree that could cause severe bradycardia by electrolyte concentration changes in the extracellular space, as frequently occurs in ESRD patients on HD.

In this study, we test this hypothesis in a computational model based on the Fabbri et al. model of human sinus node cells (10). A computational approach provides controlled conditions and allows to investigate the role of electrolyte changes on cellular sinus node pacemaking in a human setting. This is challenging experimentally

because human sinus node cells are very rarely available. Given the vastly different beating rates of commonly used laboratory animals (mouse: 500 bpm, rabbit: 300 bpm) and humans (60 bpm), it cannot be assumed that the delicate balance of competing effects on pacemaking can be transferred from animal models to humans in general and in particular during late DD, which only exists at comparatively low beating rates as typical for humans. Indeed, a computational interspecies analysis revealed fundamental differences regarding the response to extracellular ion concentration changes between human and animal (rabbit, mouse) models with a markedly higher effect in humans (11).

Our computational study yields mechanistic insight and an experimentally testable hypothesis regarding the regulation of sinus node pacemaker cell function, suggesting a pathomechanism that could be responsible for a large number of sudden bradycardic deaths in ESRD patients. To complement and substantiate our in silico findings, we analyze the statistical in vivo relation between heart rate and blood electrolyte concentration in large HD and cross-sectional populations.

MATERIALS AND METHODS

Model development and validation

The intracellular ion concentrations depend on the extracellular milieu, which is tightly controlled under physiological conditions. Therefore, it is common to consider constant $[K^+]_i$ and $[Na^+]_i$ in cyclic steady-state simulations, as proposed in the original Fabbri et al. model (10). However, when modeling the effects of altered extracellular concentrations like those occurring in ESRD patients, this assumption is not valid anymore because intracellular concentrations will respond to changes of the extracellular milieu. Therefore, we extended the original model as described in detail in (11). In brief, we considered the dynamic balance of intracellular K^+ and Na^+ concentrations as governed by their influx and efflux. Additionally, we added a small conductance calcium-activated potassium current (I_{SK}) as proposed in (12,13). Lastly, the formulation of the maximal I_{Kr} conductivity g_{Kr} was adapted to take the dependency on $[K^+]_o$ into account, as described for other cardiomyocytes (14):

$$I_{Kr} = g_{Kr} \times \sqrt{\frac{[K^+]_o}{5.4mM}} (V_m - E_K) \times (0.9paF + 0.1paS) \times piy$$

A schematic of the updated model is shown in Fig. 1. All parameters and initial values of the updated model are available, together with the unaltered equations of the original model as detailed in (10). The Loewe-Lutz-Fabbri-Severi model is available in the CellML repository (www.cellml.org). AP features of the updated model (11) were closer to experimental values than those of the original model except for AP duration (APD), AP overshoot, and the diastolic depolarization rate during the first 100 ms (DDR₁₀₀), which is higher in the updated model, leading to a more pronounced biphasic DD. The resulting model was validated against the same experimental data as the original model (10). The effect of I_f , I_{Na} , and I_{Ks} mutations was not markedly affected by the changes to the model. The response to complete I_f block (cycle length +25.9%) was in accordance with the available experimental human data (+26% (15)). In summary, the updated model exhibits

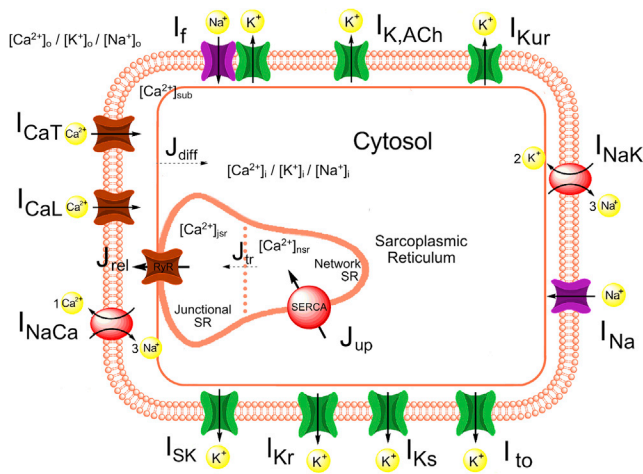


FIGURE 1 Schematic diagram of the updated human sinus node cell model. Compared to the original Fabbri et al. model (10), a small conductance calcium-activated potassium current (I_{SK}) was added, and the model took into account the dependency of g_{Kr} on $[K^+]_o$, as well as the dynamic intracellular concentration changes of not only calcium but also sodium and potassium. Details regarding the updated Loewe-Lutz-Fabbri-Severi model, including the full list of parameters and initial values, are available on www.cellml.org. To see this figure in color, go online.

homeostasis of intracellular ion concentrations across timespans of minutes and thereby puts further physiological constraints on the free parameters compared to the original version without impairing reproduction of experimental AP and calcium transient (CaT) features.

Simulation study

Based on a pilot study (16), we performed a simulation study varying the extracellular electrolyte concentrations in ranges also including the interval observed in HD patients. $[Na^+]_o$ was varied between 120 and 160 mM, $[K^+]_o$ between 3 and 9 mM, and $[Ca^{2+}]_o$ between 0.8 and 2.9 mM. The single-cell model was numerically integrated with MATLAB's (The MathWorks Inc., Natick, MA) variable-order stiff ordinary differential equation solver *ode15s*. Absolute and relative tolerances were set to $1e-6$, and the maximal allowed time step for the solver was 1 ms. Each setup was run for 100 s, after which a cyclic steady state was reached (cycle length SD for the last five beats $<0.1\%$). To disentangle the contribution of the three currents directly affected by changes of $[Ca^{2+}]_o$, namely I_{CaL} , I_{CaT} , and I_{NaCa} , we performed additional simulations in which just one of the currents was exposed to the altered $[Ca^{2+}]_o$ while the other two were computed using the reference concentration of 1.8 mM. We evaluated the following AP and CaT features for each of the simulated scenarios: cycle length, AP duration at 90% repolarization (APD_{90}), maximal diastolic potential (MDP), AP overshoot, DDR_{100} as a first-order approximation of the DD rate during the first 100 ms, maximal AP upstroke velocity dV/dt_{max} , $t_{takeoff}$ and $V_{takeoff}$ at AP takeoff identified as the first time step after $t_{MDP} + 100$ ms for which $d^2V/dt^2 > 1000$ mV/s², CaT duration at 50% (CaTD₅₀), and CaT amplitude. To study the contribution of individual currents in the different temporal phases of DD, we split this phase into early DD (first 100 ms after t_{MDP}) and late DD (the remainder). Moreover, we linearly extrapolated the effect of the first 100 ms of DD onto the whole DD phase,

$$t_{dia,100} = \frac{V_{takeoff} - MDP}{DDR_{100}}$$

and defined $t_{dia,late}$ as the remaining DD not captured by this first-order approximation based on the first 100 ms:

$$t_{dia,late} = t_{takeoff} - t_{dia,100}$$

Retrospective analysis of clinical data

To identify the in vivo relationship between heart rate and blood electrolyte concentrations, two large HD and cross-sectional populations were used. Our analysis included 741 HD patients over 4391 observations receiving chronic maintenance HD treatment for at least 3 months but not longer than 1 year. Patients that had four or more calcium and potassium measurement accompanied with an assessment of predialysis heart rate were included in the analysis. The longitudinal association was quantified using a linear mixed effects model with the additional random effect of considering the time from the first dialysis. The Western institutional review board determined this study in HD patients as exempt and in compliance with the Health Insurance Portability and Accountability Act of 1996. As an independent second population, 18,141 individuals were assessed from the 2011–2016 National Health and Nutrition Examination Survey (NHANES) US cross-sectional database (15). Appropriate sample weights were used to ensure the results are representative for the US population as a whole. In comparison to the HD patients, the NHANES study did not contain a longitudinal aspect. Therefore, a linear regression model was used. Additionally, both data sets were split into three age categories—younger than 50 years, between 50 and 69 years, and 70 years or older—and analysis was done per sex. Statistical significance was assessed by Student's *t*-test after checking for normal distributions. All results are given as mean \pm SD.

RESULTS

Hypocalcemia severely slows pacemaking in silico

The spontaneous beating cycle length of the human sinus node cell model as well as AP and CaT morphology changed when varying extracellular calcium and potassium concentrations (Fig. 2). The cycle length showed a pronounced inverse relation with the extracellular calcium concentration $[Ca^{2+}]_o$. The superlinear course, particularly for low $[Ca^{2+}]_o$, led to cycle lengths up to 2,300 ms at 0.8 mM, i.e., beating rates down to 26 bpm (Fig. 3 A). APD_{90} was shortened by both hyper- and hypocalcemia,

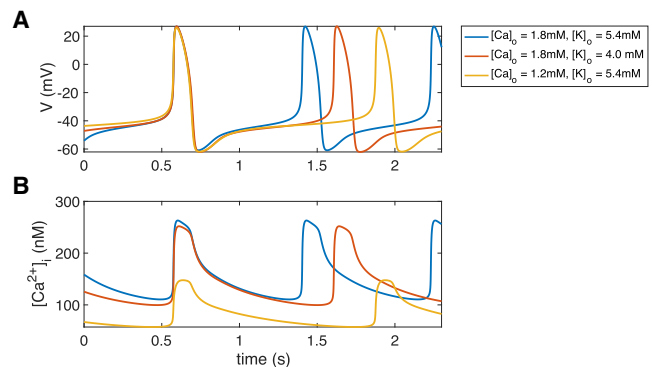


FIGURE 2 AP (A) and CaT (B) of the reference model (blue), as well as hypokalemic (red) and hypocalcemic (yellow) setups. To see this figure in color, go online.

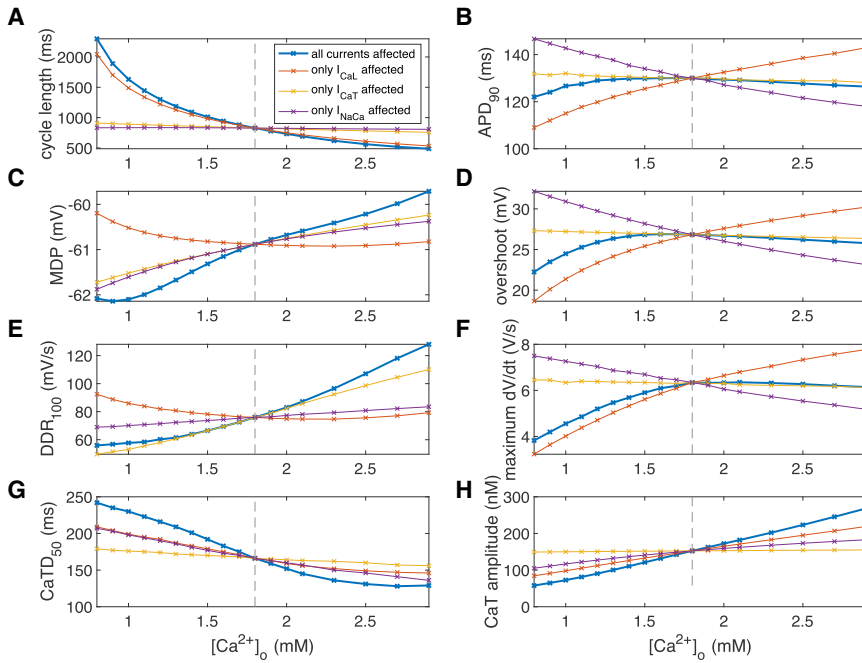


FIGURE 3 Action potential (AP) and calcium transient (CaT) feature dependency on extracellular calcium concentration $[Ca^{2+}]_o$. (A) Cycle length of spontaneous sinus node cell beating, (B) APD_{90} , (C) maximal diastolic potential, (D) AP overshoot, (E) DDR_{100} after MDP, (F) AP upstroke velocity, (G) CaT duration at 50%, and (H) CaT amplitude are shown. The thick blue line represents the scenario in which all currents were exposed to the altered $[Ca^{2+}]_o$, whereas the thin lines represent scenarios in which only one current was exposed to the altered concentration while the other two were computed with 1.8 mM. To see this figure in color, go online.

however, by less than 8 ms (Fig. 3 B), similar to AP overshoot (Fig. 3 D) and dV/dt_{max} (Fig. 3 F). MDP showed a monotonic relation with a maximal reduction of 1.2 mV at 0.8 mM $[Ca^{2+}]_o$ (Fig. 3 C), similar to DDR_{100} , which was slowed by a maximum of 20 mV/s at 0.8 mM compared to 1.8 mM $[Ca^{2+}]_o$ (Fig. 3 E). $CaTD_{50}$ was longer and CaT amplitude smaller for lower $[Ca^{2+}]_o$ (Fig. 3, G and H).

The marked hypocalcemia-induced increase in cycle length (CL) by up to 1472 ms (Fig. 4 A) was only to a minor degree caused by changes in MDP, DDR_{100} , and $V_{takeoff}$ (Fig. 4 D) as quantified by $t_{dia,100}$ (up to 203 ms, Fig. 4 B). The strongest driver of CL increase at low $[Ca^{2+}]_o$ was prolonged late DD, i.e., slowed DDR after the first 100 ms (Fig. 4 C). APD_{90} changes (up to -8 ms) mildly attenuated the hypocalcemia-induced CL increase.

Changes of $[K^+]_o$ affected spontaneous beating rate and AP morphology to a smaller degree than $[Ca^{2+}]_o$ changes. Hyperkalemia led to a mild decrease of CL up to -225 ms at 8.8 mM compared to 5.4 mM (Fig. 5 A). The tachycardic effect of hyperkalemia was mainly caused by faster late DD (Fig. 5 C) and to a lesser degree by early DD (Fig. 5 B) and APD shortening, whereas the takeoff potential was unaffected (Fig. 5 D).

Varying the extracellular sodium concentration had a minor effect on the spontaneous beating of the human sinus node cell model. Cycle length increased by only 3.9% when decreasing $[Na^+]_o$ from 140 to 120 mM and decreased by 3.9% when increasing $[Na^+]_o$ from 140 to 160 mM. Other AP features were hardly affected as well (maximal changes of 2.6 mV for overshoot, 0.18 mV for MDP, 7 ms for APD_{90} , and 2.2 mV/ms for DDR_{100}).

Attenuated late diastolic I_{CaL} and secondary attenuation of I_{NaCa} are the drivers of hypocalcemia-induced cycle length prolongation

To quantify the net effect of altered $[Ca^{2+}]_o$ on DD, we analyzed temporal means of currents for 1) the entire DD (t_{MDP} to $t_{takeoff}$), 2) early DD (t_{MDP} to $t_{MDP+100}$ ms), and 3) late DD ($t_{MDP+100}$ ms to $t_{takeoff}$) (Fig. 6). We observed an almost linear inverse relation between diastolic total transmembrane current I_{tot} and reduction of $[Ca^{2+}]_o$ (Fig. 6 Ai), particularly during late DD (Fig. 6 Aiii). The strongest contributors to this effect were I_{NaCa} (Fig. 6 Bi) and I_{CaT} (Fig. 6 Ci) as reduced inward currents, the latter particularly during early DD. Decreased outward currents I_{Kr} and I_{NaK} (Fig. 6 Di) and, to a smaller extent, I_{SK} (Fig. 6 Ei) partly counterbalanced the reduced influx.

By exposing only a single current of the three that are directly affected by changes of $[Ca^{2+}]_o$ (I_{CaL} , I_{CaT} , and I_{NaCa}) to the altered extracellular calcium concentration, I_{CaL} could be identified as the primary driver of hypocalcemia-induced CL prolongation (red lines in Figs. 3 and 4, dashed lines in Figs. 6 and 7). Even if I_{CaT} and I_{NaCa} still experienced the reference $[Ca^{2+}]_o$ of 1.8 mM, the bradycardic effect of hypocalcemia was retained almost completely (prolongation by 1261 ms vs. 1472 ms at 0.8 mM, Fig. 4 A). The contribution of I_{CaT} during early DD (Fig. 6, Aii and Cii) had only a markedly smaller effect on CL (prolongation by 83 ms at 0.8 mM, Fig. 4 A).

The mechanism by which I_{CaL} markedly prolonged CL under hypocalcemic conditions could be identified as the following: lower $[Ca^{2+}]_o$ sustainably reduced the I_{CaL}

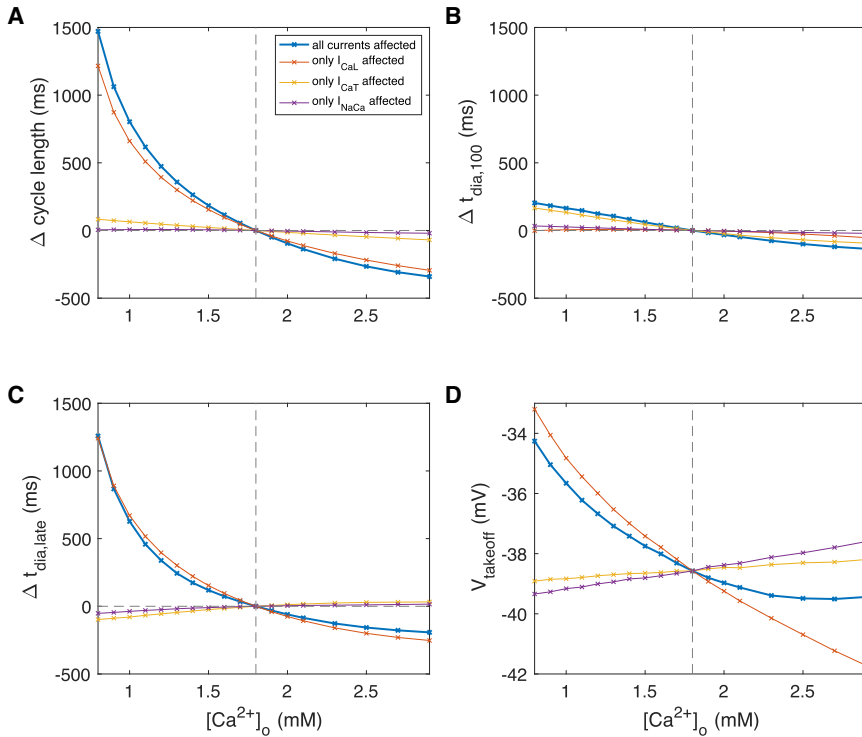


FIGURE 4 Changes of AP characteristics upon changes of extracellular calcium concentration $[Ca^{2+}]_o$. (A) Cycle length of spontaneous sinus node cell beating, (B) first-order approximation of DD time based on the first 100 ms including effects of MDP, DDR_{100} , and the takeoff potential, (C) DD time change not covered by the first-order approximation $t_{dia,100}$, and (D) AP takeoff potential are shown. The thick blue line represents the scenario in which all currents were exposed to the altered $[Ca^{2+}]_o$, whereas the thin lines represent scenarios in which only one current was exposed to the altered concentration while the other two were computed with 1.8 mM. To see this figure in color, go online.

driving force (up to twofold) and therefore its amplitude during late DD when it is active (Fig. 6 Biii). The smaller calcium influx into the intracellular and subsarcolemmal space over time led to lower concentrations there (Fig. 7,

C and D) and also in the sarcoplasmic reticulum compartments (Fig. 7, E and F). In turn, I_{NaCa} became smaller (Fig. 6 B), which led to a $[Na^+]_i$ decrease (Fig. 7 B), ending up in a new cyclic steady state. The intracellular potassium

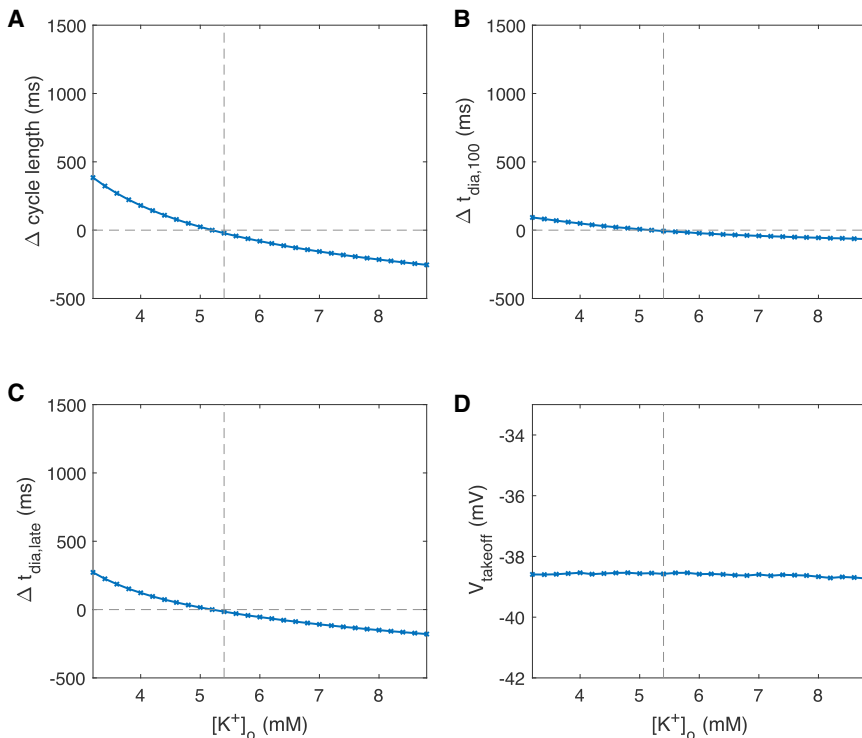


FIGURE 5 Changes of AP characteristics upon changes of extracellular potassium concentration $[K^+]_o$. (A) Cycle length of spontaneous sinus node cell beating, (B) first-order approximation of DD time based on the first 100 ms including effects of MDP, DDR_{100} , and the takeoff potential, (C) DD time change not covered by the first-order approximation $t_{dia,100}$, and (D) AP takeoff potential are shown. To see this figure in color, go online.

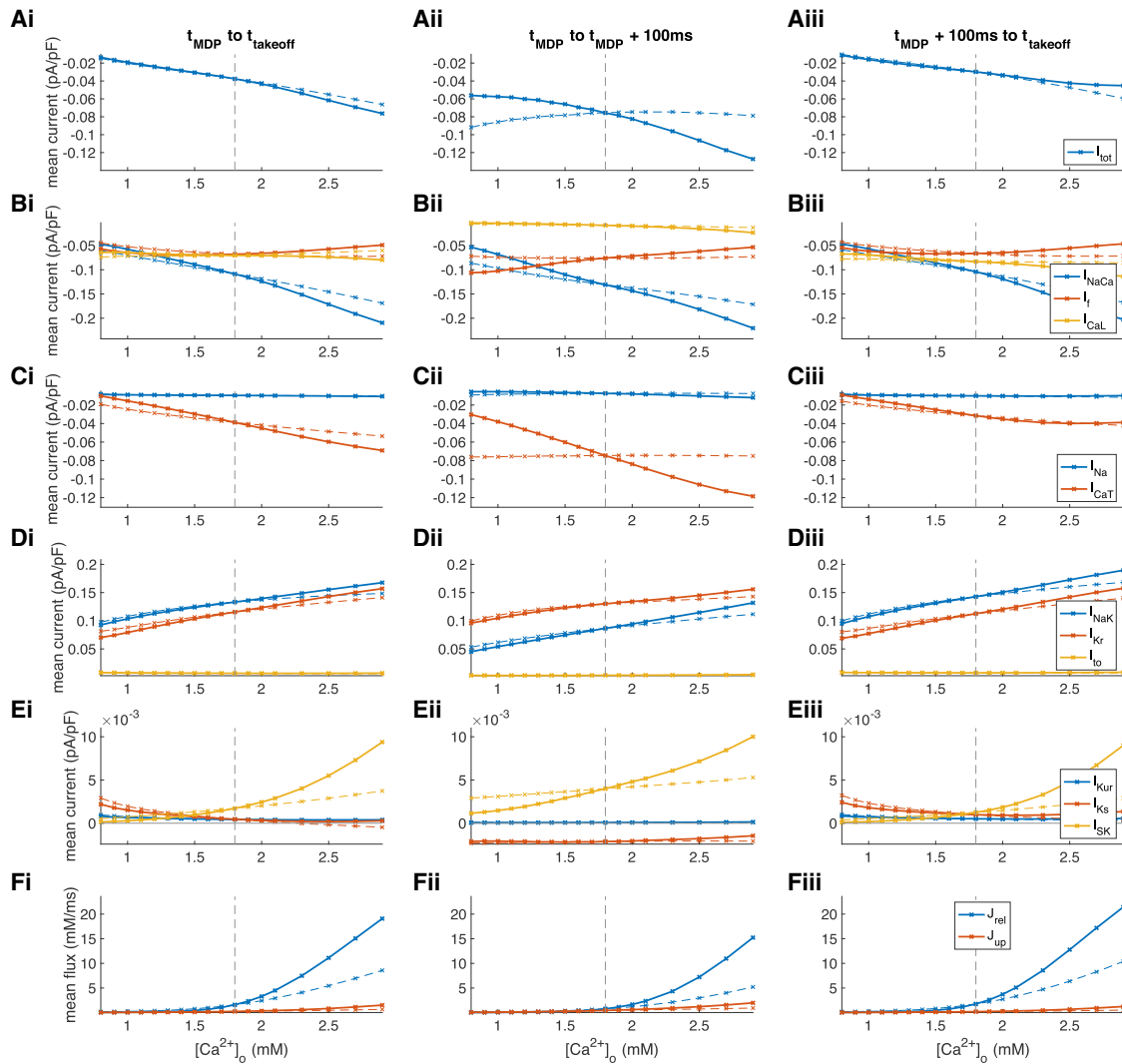


FIGURE 6 Changes of ionic current (A–E) and flux (F) mean values during DD upon changes of extracellular calcium concentration $[Ca^{2+}]_o$. (i) Mean over entire DD phase, (ii) mean over first 100 ms of DD, and (iii) mean over the late depolarization phase (excluding the first 100 ms) are shown. The solid lines represent the scenario in which all currents were exposed to the altered $[Ca^{2+}]_o$, whereas the dashed lines represent scenarios in which only I_{CaL} was exposed to the altered concentration while the other two (I_{CaT} , I_{NaCa}) were computed with 1.8 mM. To see this figure in color, go online.

concentration was not markedly affected by changes of $[Ca^{2+}]_o$ (Fig. 7 A).

Hypocalcemia is correlated with lower heart rate in vivo

As an initial validation step, we studied the empirical in vivo correlation between blood electrolyte concentrations and heart rate in two large independent populations (baseline characteristics given in Table 1). Compared to the in silico single-cell experiments, one would expect marked attenuation of the hypocalcemic effect by an intact autonomic nervous system comprising a control loop for heart rate. Indeed, we found statistically highly significant evidence of an inverse relation between total serum Ca and heart rate (Fig. 8) in both populations. In HD patients, the effect

became more pronounced with age, with no significant correlation for patients younger than 50 years, 5.35 ± 1.83 bpm/mM total Ca for 50–70 years ($p < 0.005$), and 6.32 ± 2.29 bpm/mM total Ca for individuals of age >70 years ($p < 0.01$). This age dependency was not seen in the NHANES individuals, who overall had a good renal clearance (estimated glomerular filtration rate [eGFR] (17) 102.1 ± 28.5 mL/min/1.73 m²; <15 mL/min/1.73 m² in only 0.29% of individuals). The strength of the linear dependency of total serum calcium and heart rate was more pronounced in the NHANES data across age groups: <50 years (9.63 ± 1.30 bpm/mM total Ca, $p < 0.001$), 50–70 years (8.75 ± 1.99 bpm/mM total Ca, $p < 0.001$), and >70 years (9.94 ± 2.42 bpm/mM total Ca, $p < 0.001$).

Potassium, on the other hand, had a similar inverse correlation to heart rate for all age groups in the HD

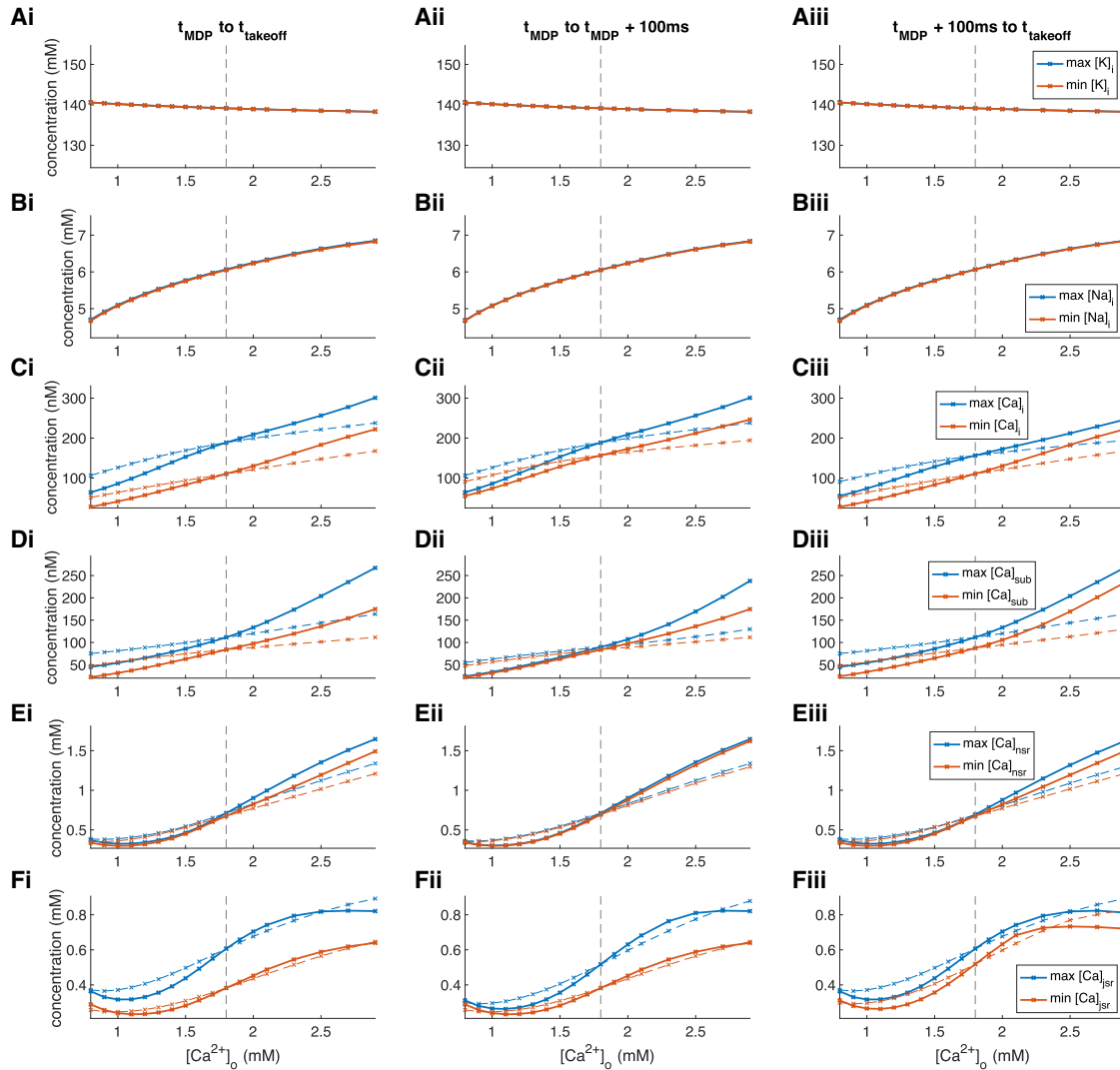


FIGURE 7 Changes of ionic concentrations (A–F) during DD upon changes of extracellular calcium concentration $[Ca^{2+}]_o$. (i) Maximal and minimal concentrations over entire DD phase, (ii) maximal and minimal concentrations over first 100 ms of DD, and (iii) maximal and minimal concentrations over the late depolarization phase (excluding the first 100 ms) are shown. The solid lines represent the scenario in which all currents were exposed to the altered $[Ca^{2+}]_o$, whereas the dashed lines represent scenarios in which only I_{CaL} was exposed to the altered concentration while the other two (I_{CaT} , I_{NaCa}) were computed with 1.8 mM. To see this figure in color, go online.

population: <50 years (-2.09 ± 0.66 bpm/mM K, $p < 0.005$), 50–70 years (-1.55 ± 0.42 bpm/mM K, $p < 0.001$), and >70 years (-1.73 ± 0.54 bpm/mM K, $p < 0.005$). The effect was similar in the NHANES individuals, with only a lower significance in the age group 50–70 years.

The bradycardic effect of hypocalcemia was markedly stronger in males, with a factor of ≈ 2 between the results for males and females seen in both the NHANES and HD populations. $[K^+]_o$ had a significant inverse correlation with heart rate in both sexes.

DISCUSSION

In this study, we tested the hypothesis that human sinus node cellular spontaneous beating rate is affected by changes in

extracellular ion concentrations like those occurring in ESRD patients undergoing HD. Using a computational model, we show that hypocalcemia has a pronounced bradycardic effect in isolated human sinus node cells with healthy electrophysiology. The beating rate was reduced by 46 bpm when reducing extracellular ionized calcium concentration $[Ca^{2+}]_o$ by 1 mM from the in vitro (and in silico) reference value of 1.8 mM. The beating rate sensitivity to changes in $[K^+]_o$ (hypokalemia) was $4.1\times$ smaller than that due to changes in $[Ca^{2+}]_o$ (hypocalcemia). Moreover, because beating rate acceleration was observed for hyperkalemia, $[K^+]_o$ changes are unlikely to contribute to the high risk of severe bradycardia toward the end of the interdialytic period, during which potassium is accumulated rather than depleted in HD patients.

TABLE 1 Characteristics of the Two Populations Used to Study the Empirical In Vivo Correlation between Electrolyte Concentrations and Heart Rate

	Number of Individuals (Observations)	% Male	Age (Years)	Heart Rate (bpm)	Total Serum Calcium (mM)	Serum Potassium (mM)
Dialysis	741 (4391)	59	63.9 ± 15.73	77.91 ± 11.29	2.22 ± 0.15	4.64 ± 0.54
<50 years	138 (815)	60	38.63 ± 9.23	84.46 ± 10.05	2.20 ± 0.16	4.75 ± 0.55
50–69 years	341 (2038)	63	61.02 ± 5.77	78.11 ± 10.65	2.22 ± 0.15	4.67 ± 0.58
≥ 70 years	262 (1538)	52	78.97 ± 6.17	74.19 ± 11.12	2.25 ± 0.13	4.53 ± 0.47
Male	436 (2594)	100	62.30 ± 16.01	78.21 ± 11.17	2.21 ± 0.15	4.67 ± 0.55
Female	305 (1797)	0	64.47 ± 15.24	77.48 ± 11.46	2.25 ± 0.14	4.59 ± 0.54
NHANES	18,141	49	43.01 ± 20.57	73.34 ± 11.96	2.36 ± 0.09	3.97 ± 0.34
<50 years	10,918	49	28.70 ± 11.39	74.78 ± 11.79	2.36 ± 0.09	3.94 ± 0.31
50 to 69 years	4917	49	59.21 ± 5.64	71.86 ± 11.94	2.35 ± 0.09	3.99 ± 0.38
≥ 70 years	2306	49	76.20 ± 3.73	69.62 ± 11.61	2.35 ± 0.10	4.10 ± 0.41
Male	8915	100	42.79 ± 20.73	71.75 ± 12.00	2.36 ± 0.09	4.03 ± 0.34
Female	9226	0	43.22 ± 20.40	74.87 ± 11.71	2.35 ± 0.09	3.92 ± 0.34

By leveraging the advantages of a computational approach, we could dissect the following mechanism underlying the pronounced bradycardic effect of reduced $[Ca^{2+}]_o$: primarily, I_{CaL} is attenuated because of reduced driving force, particularly during late depolarization, which causes a secondary reduction of calcium concentration in the intracellular compartments and subsequent attenuation of I_{NaCa} , which is also a diastolic inward current, thus causing further slowing of DD. The net bradycardic effect is the result of a delicate balance of inward and outward currents during DD and changes thereof. Although the DD integral of individual currents showed changes of up to 10 nA · ms upon changes of $[Ca^{2+}]_o$, they were partly counterbalanced by other changes, yielding a net effect on the DD integral of only 1.2 nA · ms. The slowing of spontaneous beating induced by hypocalcemia was predominantly due to changes of

late DD: only 14% of the CL increase observed at the lowest $[Ca^{2+}]_o$ could be attributed to changes of MDP, DDR_{100} , and $V_{takeoff}$. The fact that 83% of this CL increase was retained when only I_{CaL} was affected by the change of $[Ca^{2+}]_o$ highlights the key role of late diastolic I_{CaL} in hypocalcemia-induced slowing of sinus node pacemaking.

Although we further constrained the human sinus node cell model by posing the physiological constraint of homeostasis, there still is a degree of uncertainty because of sparse experimental data. Therefore, experimental validation of our in silico-derived hypothesis is desirable. However, such experiments would need to be performed using human sinus node cells because of crucial interspecies differences in the response of sinus node cells to changes of $[Ca^{2+}]_o$ (11). We could show that rabbit experimental data matches well with rabbit model predictions of

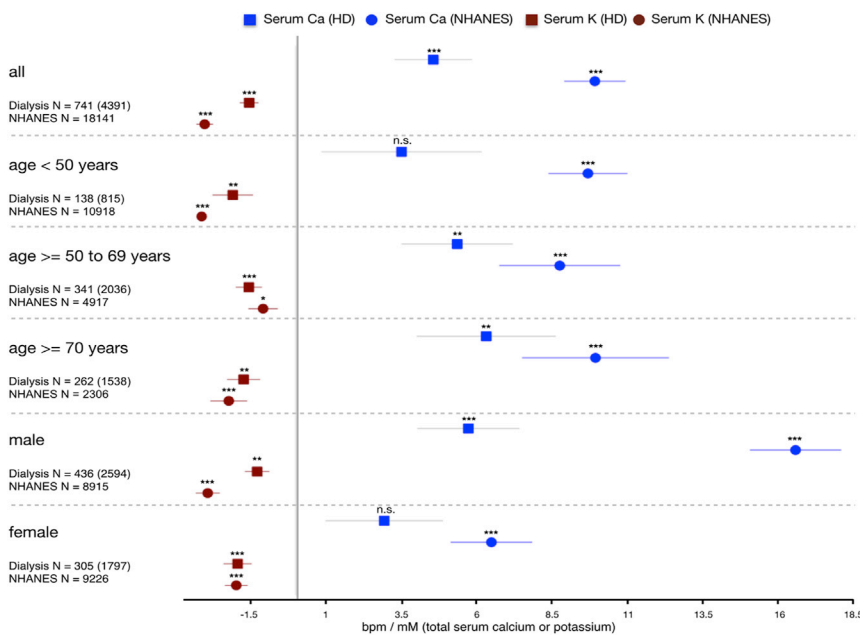


FIGURE 8 Forest plot of linear dependency between total serum calcium (blue) and potassium (red) concentrations and in vivo heart rate. Data from a linear mixed effects model of 741 hemodialysis patients (4391 observations) are indicated by squares, and circles represent a linear regression of 18,145 individuals from the NHANES cross-sectional study representative of the US population. To see this figure in color, go online.

the effect of hypocalcemia both qualitatively and quantitatively, but the effect is less pronounced by a factor of ≈ 10 compared to human sinus node cells (11). Considering that the bradycardic effect of hypocalcemia observed here was mainly due to changes in late DD (beyond 100 ms), the interspecies differences are scarcely surprising, given that this phase is not present in species with high baseline heart rate as is typical for common laboratory animals. The effect on early depolarization was comparable across species (11).

Therefore, we decided to substantiate and complement our *in silico* findings by studying the empirical correlation between heart rate and serum total calcium in two large populations. We found statistically highly significant correlations in both the HD as well as the NHANES populations in qualitative agreement with the model predictions for calcium but not potassium. The mismatch for potassium might indicate that the square-root formulation underestimates the degree of modulation of g_{Kr} by $[K^+]_o$ and could imply that hyperkalemic conditions, as is typical for the later interdialytic period, exacerbate the bradycardic effect of hypocalcemia. The bradycardic effect of hypocalcemia was increasingly stronger with higher age for the HD population, which could be an indication of a gradual loss of function of the autonomic control of heart rate with age in this population experiencing chronic sympathetic overactivity driven by afferent sensory renal nerves stimulated by renal injury (4,18). Surprisingly, the effect was stronger in the healthier NHANES population than in the HD population. A potential reason could be the smaller magnitude of calcium excursion and therefore also heart rate in the healthier NHANES population (Fig. 9), which might not cause immediate counteraction by the autonomic nervous system. To quantitatively relate these *in vivo* results with the cellular *in silico* results, the relation between $[Ca^{2+}]_o$ and total serum calcium is important. The distribution of free cations in the vascular, *i.e.*, serum, and interstitial, *i.e.*, extracellular, compartments has been reported to agree with Donnan theory predicting a ratio of 0.98 (19). Moreover, around 45% of the total serum calcium is free ionized calcium, whereas the rest is complexed or bound. Taken

together, this yields a factor of ≈ 2.27 . Thus, the overall linear effect in the NHANES population of 9.9 bpm/mM total calcium relates to an effect of ≈ 21.56 bpm/mM $[Ca^{2+}]_o$. This *in vivo* effect is about half as strong as the observed *in silico* effect, whose linear regression would likely be smaller than the factual value of 46 bpm/mM $[Ca^{2+}]_o$, assuming sampling of the superlinear course centered around the reference value. However, it should not be forgotten that the empirical data were acquired *in vivo*, *i.e.*, in a setting where the heart rate is tightly controlled through various feedback loops via the autonomic nervous system, which should to a high degree compensate changes of basal cellular beating rate caused by changes of $[Ca^{2+}]_o$. Considering this, it rather seems surprising that the *in vivo* effect is not even smaller.

Our study presents a potential mechanism contributing to SCD in ESRD patients: although in a subject with normal renal function, calcium concentrations are generally stable, the course of calcium during the interdialytic period is highly variable, and HD patients may experience relevant changes in serum calcium levels during the dialysis session. In particular, significant intradialytic reductions in calcium levels can occur if low-calcium dialysis baths (*e.g.*, 1.25 mM) are used. Dialysates with low Ca^{2+} concentrations are also associated with a higher risk of intradialysis sudden cardiac arrest (20). The patients developing hypocalcemia over the course of the interdialytic days will experience a lower basal sinus node beating rate, which would normally be counterbalanced by an increase in sympathetic tone. However, a sudden loss of sympathetic tone, as systematically observed in mouse models of ESRD (21), will unmask the lower basal sinus node beating rate, similar to those resulting from simulations not taking into account autonomic control, and cause extreme bradycardia and eventually asystole within seconds to minutes, as reported for bradycardic sudden death in HD patients (22), if secondary pacemakers cannot take over.

This hypothesis is in line with a recent epidemiological study comprising 28,471 dialysis patients (23), showing that ESRD patients on HD have an almost $6\times$ increased incidence of requiring pacemaker insertion compared to

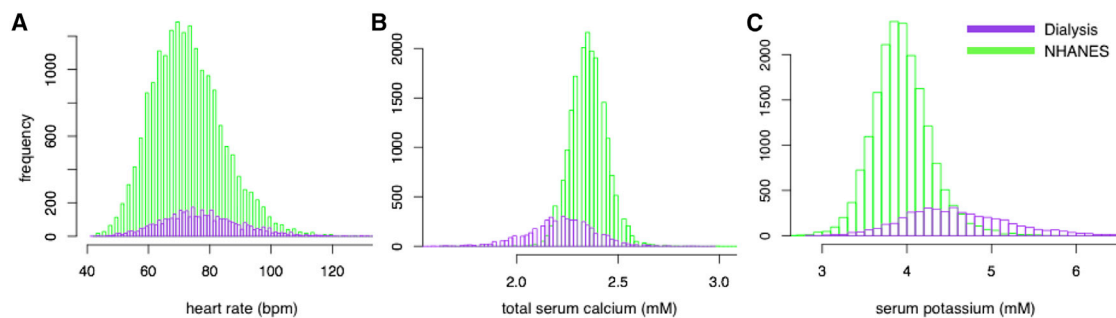


FIGURE 9 Histogram of heart rate (A), total serum calcium (B), and serum potassium (C) distributions in the NHANES and hemodialysis populations. To see this figure in color, go online.

matched patients with normal kidney function. Of note, all of the four patients suffering SCD in the study by Sacher et al. (22) had a preserved ejection fraction, suggesting that the fatal arrhythmia was not due to an underlying severe heart disease. Moreover, all of them had a record of diabetes mellitus, which is associated with autonomic neuropathy, compared to only 55% of those patients alive at the end of the follow-up period. If the crucial role of hypocalcemia is confirmed, continuous noninvasive remote monitoring of the blood calcium level using electrocardiogram [ECG]-derived features (24,25) could help to reduce SCD incidence. In addition, one could envision to explore ways to pharmacologically modulate I_{CaL} to reduce dependence on $[Ca^{2+}]_o$, thus yielding a more robust pacemaking behavior over a wider range of extracellular calcium concentrations, including hypocalcemic conditions. In this context, the role of calcium channel blockers that are widely used in ESRD patients and affect myocytes as well as blood vessels should be investigated in light of our hypothesis. In particular, the nondihydropyridine-type blockers that bind preferentially to L-type channels in the cardiac muscles appear interesting, and a negative chronotropic effect in line with our findings has been reported (26).

Limitations

Several limitations pertain to this study: 1) the *in silico* reference concentrations reflect standard *in vitro* conditions but not physiological *in vivo* concentrations. In particular, ionized calcium has been reported to vary in the range 0.9–1.6 mM in HD patients (27). The historical reasons and potential implications of this mismatch for calcium were discussed by Severi et al. (28). For the study presented here, one should refrain from taking absolute calcium concentrations into consideration and rather interpret the results in terms of concentration changes. Interestingly, the sensitivity of beating rate to calcium changes (slope of the curve in Fig. 4 A) becomes steeper in a physiological or parapsychological range ($[Ca^{2+}]_o < 1.5$ mM), and even more in conditions of pronounced hypocalcemia. 2) The uremic milieu in HD patients has been shown to affect cellular electrophysiology, as reviewed in (7). These changes have not been taken into consideration here because it is not clear how they pertain to sinus node cardiomyocytes. Also, we did not consider changes of ion channel properties due to changes of surface charge related to varying $[Ca^{2+}]_o$ (29,30). 3) Spontaneous cellular pacemaking is a necessary but not sufficient condition for the initiation of a heartbeat. In addition, the ensemble of sinus node cells needs to drive the surrounding working myocardium, which captures the excitation. This aspect will be considered in future work based on a preliminary study (31). 4) The role of the autonomic nervous system has not been considered. Although the Fabbri et al. model features sympathetic stimulation, it is only available as a binary on/off switch and beyond the

scope of this study. Future work will extend the model to allow for a gradual sympathetic response, allowing for assessment of how intact autonomic control could compensate for hypocalcemia-induced lower basal beating rate. 5) This study is based on the Fabbri et al. model of a human sinus node cell (10). Inherent sinus node heterogeneity and variability has not been considered here and is currently limited by the amount of available experimental recordings. Nevertheless, a population of models approach (32) appears desirable for the future. 6) Sympathetic hyperactivity is a frequent phenomenon in ESRD patients (18), and future studies should extend the statistical analysis to comorbidities that are associated with autonomic neuropathy to consider these potential additional confounding factors beyond age.

CONCLUSION

We derived an experimentally testable hypothesis of a pathomechanism underlying the high rate of sudden bradycardic deaths in HD patients. Our computational study suggests that a reduction of extracellular calcium concentration slows down cellular sinus node pacemaking severely by attenuation of I_{CaL} and secondarily by attenuation of I_{NaCa} during late DD. Although normally compensated by a higher sympathetic tone, a sudden loss of sympathetic tone could unmask the low basal sinus node beating rate under hypocalcemic conditions and cause extreme bradycardia. The combination of these two mechanisms (sudden loss of sympathetic tone under hypocalcemic conditions) could cause bradycardic SCD and contribute to the high prevalence of SCD in HD patients. The mechanistic *in silico* study is complemented with an *in vivo* analysis comprising >20,000 observations, which supports the computational findings. Our results could be a crucial first step to elucidate the pathomechanism behind the unexplained high rate of SCD in HD patients and eventually help to reduce its incidence.

AUTHOR CONTRIBUTIONS

A.L. and S.S. conceived the presented idea. A.L., S.S., D.H.F., P.K., J.G.R., and A.V. designed the experiments. Y.L., N.N., N.T., D.N., X.Y., J.G.R., and A.L. performed the experiments and analyzed the results. A.L., Y.L., D.N., N.N., A.F., P.K., S.G., J.G.R., and S.S. contributed to the interpretation of the results. A.L., Y.L., and D.N. drafted the manuscript. All authors provided critical feedback on, contributed to, and approved of the final manuscript.

ACKNOWLEDGMENTS

A.L. gratefully acknowledges financial support by the Ministerium für Wissenschaft, Forschung und Kunst Baden-Württemberg through the Research Seed Capital program and by the Deutsche Forschungsgemeinschaft (German Research Foundation), project ID 258734477-SFB 1173 and through grant LO 2093/1-1 project ID 391128822. N.N. acknowledges support by the National Research Development and Innovation Office

(PD-125402 and FK-129117). P.K., X.Y., and J.G.R. are employees of the Renal Research Institute, a wholly owned subsidiary of Fresenius Medical Care (FMC). D.H.F. is an employee of FMC. P.K. holds stock in FMC and receives author honoraria from UpToDate.

REFERENCES

1. Yaniv, Y., E. G. Lakatta, and V. A. Maltsev. 2015. From two competing oscillators to one coupled-clock pacemaker cell system. *Front. Physiol.* 6:28.
2. Tsutsui, K., O. Monfredi, ..., E. G. Lakatta. 2018. Self-organization of functional coupling between membrane and calcium clock in arrested human sinoatrial nodal cells in response to camp. *Biophys. J.* 114:622a.
3. Hill, N. R., S. T. Fatoba, ..., F. D. Hobbs. 2016. Global prevalence of chronic kidney disease - a systematic review and meta-analysis. *PLoS One.* 11:e0158765.
4. Di Lullo, L., R. Rivera, ..., C. Ronco. 2016. Sudden cardiac death and chronic kidney disease: from pathophysiology to treatment strategies. *Int. J. Cardiol.* 217:16–27.
5. Makar, M. S., and P. H. Pun. 2017. Sudden cardiac death among hemodialysis patients. *Am. J. Kidney Dis.* 69:684–695.
6. Wong, M. C., J. M. Kalman, ..., J. B. Morton. 2015. Temporal distribution of arrhythmic events in chronic kidney disease: highest incidence in the long interdialytic period. *Heart Rhythm.* 12:2047–2055.
7. Poulidakos, D., K. Hnatkova, ..., M. Malik. 2019. Sudden cardiac death in dialysis: arrhythmic mechanisms and the value of non-invasive electrophysiology. *Front. Physiol.* 10:144.
8. Tereshchenko, L. G., and N. G. Posnack. 2019. Does plastic chemical exposure contribute to sudden death of patients on dialysis? *Heart Rhythm.* 16:312–317.
9. Kalra, P. A., D. Green, and D. Poulidakos. 2018. Arrhythmia in hemodialysis patients and its relation to sudden death. *Kidney Int.* 93:781–783.
10. Fabbri, A., M. Fantini, ..., S. Severi. 2017. Computational analysis of the human sinus node action potential: model development and effects of mutations. *J. Physiol.* 595:2365–2396.
11. Loewe, A., Y. Lutz, ..., S. Severi. 2019. Inter-species differences in the response of sinus node cellular pacemaking to changes of extracellular calcium. *bioRxiv* <https://doi.org/10.1101/771972>.
12. Kennedy, M., D. M. Bers, ..., D. Sato. 2017. Dynamical effects of calcium-sensitive potassium currents on voltage and calcium alternans. *J. Physiol.* 595:2285–2297.
13. Fabbri, A., M. Paci, ..., S. Severi. 2017. Effects of the small conductance calcium-activated potassium current (IsK) in human sinoatrial node. *In Computing in Cardiology 2017, vol. 44. IEEE*, pp. 1–4.
14. Severi, S., D. Pogliani, ..., S. Genovesi. 2010. Alterations of atrial electrophysiology induced by electrolyte variations: combined computational and P-wave analysis. *Europace.* 12:842–849.
15. Verkerk, A. O., R. Wilders, ..., H. L. Tan. 2007. Pacemaker current (I_f) in the human sinoatrial node. *Eur. Heart J.* 28:2472–2478.
16. Loewe, A., Y. Lutz, ..., S. Severi. 2018. Severe sinus bradycardia due to electrolyte changes as a pathomechanism of sudden cardiac death in chronic kidney disease patients undergoing hemodialysis. *Heart Rhythm.* 15:S354–S355.
17. Inker, L. A., C. H. Schmid, ..., A. S. Levey; CKD-EPI Investigators. 2012. Estimating glomerular filtration rate from serum creatinine and cystatin C. *N. Engl. J. Med.* 367:20–29.
18. Kotanko, P. 2006. Cause and consequences of sympathetic hyperactivity in chronic kidney disease. *Blood Purif.* 24:95–99.
19. Gilányi, M., C. Ikrényi, ..., A. G. Kovách. 1988. Ion concentrations in subcutaneous interstitial fluid: measured versus expected values. *Am. J. Physiol.* 255:F513–F519.
20. Pun, P. H., J. R. Horton, and J. P. Middleton. 2013. Dialysate calcium concentration and the risk of sudden cardiac arrest in hemodialysis patients. *Clin. J. Am. Soc. Nephrol.* 8:797–803.
21. Zhao, Y., N. X. Chen, ..., P. S. Chen. 2016. Subcutaneous nerve activity and mechanisms of sudden death in a rat model of chronic kidney disease. *Heart Rhythm.* 13:1105–1112.
22. Sacher, F., L. Jesel, ..., C. Combe. 2018. Cardiac rhythm disturbances in hemodialysis patients: early detection using an implantable loop recorder and correlation with biological and dialysis parameters. *JACC Clin. Electrophysiol.* 4:397–408, Published online September 27, 2017.
23. Wang, I. K., K. H. Lin, ..., F. C. Sung. 2016. Permanent cardiac pacing in patients with end-stage renal disease undergoing dialysis. *Nephrol. Dial. Transplant.* 31:2115–2122.
24. Pilia, N., O. Dössel, ..., A. Loewe. 2017. ECG as a tool to estimate potassium and calcium concentrations in the extracellular space. *In Computing in Cardiology 2017, vol. 44. IEEE*, pp. 1–4.
25. Corsi, C., M. Cortesi, ..., S. Severi. 2017. Noninvasive quantification of blood potassium concentration from ECG in hemodialysis patients. *Sci. Rep.* 7:42492.
26. Mugendi, G. A., G. F. Strippoli, ..., T. M. Esterhuizen. 2014. Calcium channel blockers for people with chronic kidney disease requiring dialysis. *Cochrane Database Syst. Rev.* (4) CD011064. <https://doi.org/10.1002/14651858.CD011064>.
27. Genovesi, S., C. Dossi, ..., M. Stramba-Badiale. 2008. Electrolyte concentration during haemodialysis and QT interval prolongation in uraemic patients. *Europace.* 10:771–777.
28. Severi, S., C. Corsi, and E. Cerbai. 2009. From in vivo plasma composition to in vitro cardiac electrophysiology and in silico virtual heart: the extracellular calcium enigma. *Philos. Trans. A Math. Phys. Eng. Sci.* 367:2203–2223.
29. Hille, B., A. M. Woodhull, and B. I. Shapiro. 1975. Negative surface charge near sodium channels of nerve: divalent ions, monovalent ions, and pH. *Philos. Trans. R. Soc. Lond. B Biol. Sci.* 270:301–318.
30. Coronado, R., and H. Affolter. 1986. Insulation of the conduction pathway of muscle transverse tubule calcium channels from the surface charge of bilayer phospholipid. *J. Gen. Physiol.* 87:933–953.
31. Fabbri, A., A. Loewe, ..., S. Severi. 2017. Pace-and-drive of the human sinoatrial node - a preliminary computational investigation. *In Computing in Cardiology 2017, vol. 44. IEEE*, pp. 1–4.
32. Britton, O. J., A. Bueno-Orovio, ..., B. Rodriguez. 2013. Experimentally calibrated population of models predicts and explains intersubject variability in cardiac cellular electrophysiology. *Proc. Natl. Acad. Sci. USA.* 110:E2098–E2105.